Available online at www.sciencedirect.com
SCIENCE DIRECT®
Journal of Sound and Vibration 278 (2004) 1051–1080
JOURNAL OF SOUND AND VIBRATION
www.elsevier.com/locate/jsvi

A unified control framework of the non-regular dynamics of mechanical oscillators

S. Lenci[a], G. Rega[b,*]

[a] *Istituto di Scienza e Tecnica delle Costruzioni, Università Politecnica delle Marche, via Brecce Bianche, Ancona 60131, Italy*
[b] *Dipartimento di Ingegneria Strutturale e Geotecnica, Università di Roma "La Sapienza", via A. Gramsci 53, Roma 00197, Italy*

Received 13 May 2003; accepted 22 October 2003

Abstract

A method for controlling non-linear dynamics and chaos based on avoiding homo/heteroclinic bifurcations is considered in a unified framework. Various non-linear oscillators, both hardening and softening, symmetric and asymmetric, considered as archetypes of a more general class of single-d.o.f. systems, are analyzed. The Melnikov's method is applied to analytically detect the homo/heteroclinic bifurcations, and the results are used to select the optimal shape of the excitation permitting the maximum shift of the undesired bifurcations in parameter space. The *generic* character of the *optimization problem* is highlighted, and the problem itself is discussed in detail. Various control strategies are proposed, based on the elimination either of a single bifurcation (one-side controls) or of all bifurcations (global control). The optimization problems are solved, analytically and numerically, under various forms, by taking into account the physical admissibility of the related optimal excitation and the easiness of implementation in practical applications. It is shown that the *solutions* of one-side control problems are always *system independent*. In turn, the solutions of global control problems are system independent for the large class of (symmetric) systems considered in this work, although there are other systems whose solutions are system dependent. These considerations support the very generic nature of the *optimal control*.

1. Introduction

In the last decades there has been a growing attention to the study of non-linear dynamics of various mechanical systems. From a practical point of view, this interest was motivated by the

*Corresponding author. Fax: +39-06-322-1449.
E-mail addresses: lenci@univpm.it (S. Lenci), giuseppe.rega@uniroma1.it (G. Rega).

0022-460X/$ - see front matter © 2003 Elsevier Ltd. All rights reserved.
doi:10.1016/j.jsv.2003.12.010

need to analyze the dynamic behaviour of more and more refined high-performance structures, usually employed in severe operating conditions. These mechanical systems have to be designed with the aim of reducing the amount of employed material to the minimum, and they are usually lighter and more slender than the old ones. For such structures, linear analysis is no longer sufficient to capture the main behaviours, and a non-linear analysis is required.

Fortunately enough, these growing engineering requirements were paralleled by a notable advance in dynamical systems theory, which permitted discovery, analysis and successive detection of several typical phenomena of the non-linear range playing a fundamental role in the behaviour of many mechanical systems. Concepts like "non-linear resonance", "bifurcation" and "chaos" are by now well understood by many researchers in the mechanics community. Indeed, the application of the abstract theory of dynamical systems to mechanics represents one important achievement of recent years and a well-defined research field.

Proper design or control of these "non-linear" structures requires the knowledge of the non-linear phenomena with respect to which the performances should be optimized. Thus, the analysis of given non-linear dynamics of different mechanical systems, largely investigated in the past years (see, e.g., Refs. [1–4]), is the necessary background upon which it is actually possible to develop strategies for optimizing the system properties and response. In this respect, different systems sharing the same non-linear phenomena are expected to exhibit a common underlying theoretical behaviour, entitled to become practically meaningful in all situations wherein the considered phenomena are important for the system.

One scope of the present paper consists in investigating whether a *generic* dynamic behaviour can entail a *generic* approach to control—or design—of mechanical systems. As a matter of fact, if the control is based on the peculiarities of a fundamental non-linear dynamic property and not on the specific characteristics of the system, it may be expected that the same ideas and methods developed to control one system should be effective for all systems sharing the same property, the differences being of minor relevance and possibly of technical nature. Thus, the efforts paid in the non-linear analysis of various mechanical systems, which is a difficult task usually leading to the identification of common non-linear behaviours, may be compensated by the possibility to develop unified control methods and techniques, with all the advantages of having a well-defined and common framework, and with the possibility of establishing important analogies between different mechanical systems.

Attention is focused on the homo/heteroclinic bifurcations of selected hilltop saddles. This is motivated by the fundamental role played by this global bifurcation in non-linear dynamics, as noted, e.g., by Kovacic and Wiggins [5] according to which "...it is not an exaggeration to claim that in virtually every manifestation of chaotic behaviour known thus far, some type of homoclinic behaviour is lurking in the background...". This observation has been repeatedly confirmed in practice (see, e.g., Refs. [6,7]), in various circumstances and for different systems. In fact, homo/heteroclinic bifurcations are certainly responsible for fractalization of the boundaries of basins of attractions, for sensitivity to initial conditions, for chaotic transients and for the appearing/disappearing of invariant chaotic sets constituted by infinitely many unstable periodic and aperiodic orbits, which largely influence the overall dynamics and often constitute the skeleton of chaotic attractors [8–10]. Furthermore, they may be responsible for the creation, widening or splitting of a chaotic attractor, for the erosion of safe basin [11], and they are involved in the escape from potential wells [12,13].

Based on previous observations, the idea for controlling non-linear dynamics is that of eliminating or, better, properly shifting in parameter space, the homo/heteroclinic bifurcation of the relevant hilltop saddle, thus contributing to the removal of the non-linear phenomena previously mentioned. This objective can be pursued in various manners [14–16] and, among others, the modification of the shape of the excitation is chosen, i.e., the amplitude and frequency are fixed and only the shape is allowed to vary in order to eliminate the global bifurcation as far as possible. The proposed method has been applied with some success to an inverted piecewise linear pendulum with rigid lateral barriers [17,18] and to specific smooth non-linear systems [13,19]. In these works the main ideas are explained, the optimal shapes are obtained and systematic numerical analyses are performed to confirm the theoretical predictions and the practical effectiveness of the method.

The present paper generalizes previous separate achievements. It is aimed (i) at applying the control to a wider class of *smooth* mechanical systems where the homo/heteroclinic bifurcations play an important role, and (ii) at pointing out and studying in detail the generic character of the proposed method and its *unifying* features. Attention is focused on one-degree-of-freedom (1-d.o.f.) oscillators representing either real mechanical models or unimodal approximations of the dynamics of non-resonant continuous systems. More precisely, the class of oscillators

$$\ddot{x} + \varepsilon\delta\dot{x} + F(x) = \varepsilon\gamma(\omega t), \tag{1a}$$

$$\gamma(s) = \sum_{j=1}^{\infty} \gamma_j \sin(js + \Psi_j), \tag{1b}$$

is investigated. In Eq. (1) $F(x)$ is the non-linear restoring force characterizing different mechanical behaviours, $\varepsilon\delta$ the viscous damping, $\varepsilon\gamma(\omega t)$ the generic T-periodic ($T = 2\pi/\omega$) external excitation and ε a dimensionless smallness parameter introduced to emphasize the smallness of damping and excitation.

The number of homo/heteroclinic orbits of the unperturbed undamped (i.e., $\varepsilon = 0$) version of Eq. (1) depend on the function $F(x)$, and their existence can be shown, for example, by the method developed by Lenci and Lupini [20]. The homo/heteroclinic bifurcations are detected by the Melnikov's method [8–10], which is a useful mathematical tool permitting analytical computations. It allows for an analytical approach to the problem, and, consequently, for an overall, quite systematic, investigation.

The more general case of coexistence of parametric and external excitations can be transformed in the case of equivalent external excitation just as done in Ref. [13] for the Helmholtz oscillator. In turn, the case of quasi-periodic external/parametric excitations only requires extended versions of the Melnikov's method (see, for example, Refs. [9,21]) and major efforts in computing the Melnikov's function, but basically it does not affect the control method. It has been addressed, e.g., by Lima and Pettini [14] for the Duffing equation. The extension to continuous systems, on the other hand, can be performed analogously in several cases by a further extension of the Melnikov's method due to Holmes and Marsden [22], which permits the analytical detection of the global bifurcation also in the case of infinite dimensional dynamical systems. All of these generalizations involve mostly technical aspects, sometimes of minor importance, and the principal features of non-regular dynamics and control are illustrated and discussed in this work without too much loss of generality, although some further developments can be already foreseen.

The paper is organized as follows. In the following section the Melnikov analysis permitting a theoretical prediction of global bifurcations is performed for both softening (Section 2.1) and hardening (Section 2.2) oscillators. The optimal problems required to detect the best shape of the excitation are also stated in Section 2, while they are analyzed and solved under various forms in Section 3. In particular, two different control classes are identified and considered: (i) one-side control (Section 3.1)—i.e., elimination of a single homo/heteroclinic bifurcation; (ii) global control of symmetric systems (Section 3.2) — i.e., simultaneous elimination of two global bifurcations. It is shown that there is a *single* mathematical *problem* of optimization, unconstrained in the case of one-side control (Eq. (45)) and constrained in the case of global control (Eq. (59)). Moreover, in the case of one-side control the *solution* is always *system independent*, as it does for the global control of the large class of considered systems. This highlights the very generic nature of the control method and, in particular, it shows how the common dynamical event addressed (homo/heteroclinic bifurcations) entails unifying properties of the control method, irrespective of the actually considered mechanical system.

A different situation occurs in the case of global control of asymmetric hardening systems. In this case, the optimization problems maintain some kind of generality, thus confirming the unified control framework, but the solutions are system dependent. This requires a more involved analysis—though less general than that reported in this paper—which is discussed in Ref. [23] for the case of the hardening Helmholtz–Duffing oscillator.

2. Global bifurcations and control strategy in various 1-d.o.f. systems

With the aim of showing the generic character of control and its "independence" of the specific mechanical nature of the system, both softening (Section 2.1) and hardening (Section 2.2), symmetric and asymmetric, oscillators are considered. However, in order to be concrete and specific, only few *representative* cases are analyzed for each class of systems.

2.1. Softening oscillators

2.1.1. Helmholtz equation: the single-well potential with one escape direction

The standard Helmholtz oscillator

$$\ddot{x} + \varepsilon\delta\dot{x} - x + x^2 = \varepsilon\gamma(\omega t), \tag{2}$$

which is a special case of Eq. (1) obtained assuming $F(x) = -x + x^2$, is considered in this subsection. The Helmholtz equation (2), whose potential $V(x) = -x^2/2 + x^3/3$ and unperturbed phase space are reported in Figs. 1a and b, respectively, is an archetype for the study of smooth non-linear oscillators with only one escape direction. It governs the dynamics of various mechanical systems, such as, e.g., prestressed membranes, rolling asymmetric ships, asymmetric cranes, etc. [13]. In spite of its seeming simplicity, it has a very complex dynamics showing several non-linear phenomena, such as non-linear resonance, multistability, chaotic and regular dynamics, various kinds of local and global bifurcations. From a practical point of view, a very important aspect is the escape from the potential well, a phenomenon which leads to system unserviceability (for example, ship capsizing) or structural failure. This aspect has been

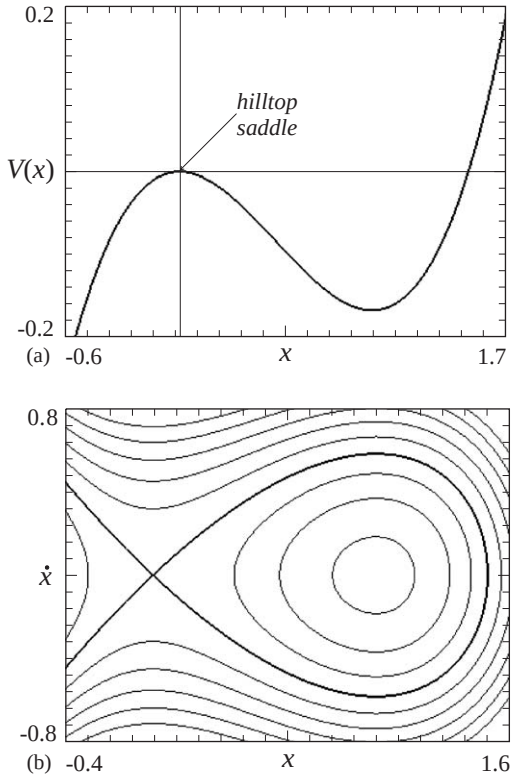

Fig. 1. (a) The potential $V(x)$ and (b) the unperturbed phase space of the Helmholtz equation (2).

extensively studied in the past (see, for example, Refs. [12,24,25]) and it has been controlled by the authors [13] using the method discussed herein. Accordingly, this section simply summarizes the results reported in Ref. [13], where the complete analysis and detailed numerical simulations showing the practical effectiveness of the method can be found.

In the unperturbed undamped dynamics of Eq. (2), there are two equilibrium points $x_1 = 0$, which is the unique hilltop saddle, and $x_2 = 1$, which is a centre. The saddle has a (right) homoclinic orbit

$$x_{hom}(t) = \frac{3}{2}\frac{1}{\cosh^2(t/2)} \tag{3}$$

surrounding the unique potential well, while the other (left) stable and (left) unstable manifolds diverge to infinity. The homoclinic loop separates the bounded periodic oscillations from the unbounded trajectories, and when the excitation is added it splits into two manifolds which may or may not intersect depending on the relative magnitude of the excitation amplitude and damping. More precisely, for low values of amplitude the damping keeps the manifolds separated, while for large values of amplitude the intersection takes place. There exist intermediate critical values corresponding to homoclinic bifurcations [8], which can be analytically computed by the Melnikov's method.

The application of this method to Eq. (2) is standard, and the Melnikov's function representing the first order approximation (in ε) of the signed distance between stable and unstable manifolds is given by

$$\mathtt{M}(m) = \int_{-\infty}^{\infty} \dot{x}_{hom}(t)[-\delta \dot{x}_{hom}(t) + \gamma(\omega t + m)]\,\mathrm{d}t. \tag{4}$$

Computing the integrals in Eq. (4) by the residues method leads to the following expression of the Melnikov function [13]:

$$\mathtt{M}(m) = -\frac{6}{5}\left[\delta + \gamma_1 \frac{5\pi\omega^2}{\sinh(\omega\pi)} h(m)\right], \tag{5}$$

where

$$h(m) = \sum_{j=1}^{\infty} h_j \cos(jm + \Psi_j), \quad h_j = \frac{\gamma_j}{\gamma_1} \frac{j^2 \sinh(\omega\pi)}{\sinh(j\omega\pi)}. \tag{6a, b}$$

Note that $h_1 = 1$ and that $h(m)$ is 2π-periodic and has zero mean value.

Expression (5) is written in such a way to give γ_1 the role of overall *amplitude*. The remaining dimensionless parameters γ_j/γ_1 obtained from Eq. (6b) simply govern the *shape* of the excitation, namely, they measure the superharmonic corrections to the basic harmonic excitation. In terms of Melnikov function, the effects of such corrections are governed by the parameters h_j, $j > 1$, contributing to the "amplitude-free" oscillating part $h(m)$ of the distance between the manifolds.

Apart from the unessential factor $-\frac{6}{5}$, expression (5) shows how the distance is actually composed of two parts, the constant part δ and the oscillating part $h(m)$ multiplied by its amplitude $\gamma_1 5\pi\omega^2/\sinh(\omega\pi)$. Remembering that the Melnikov function represents the distance to the first order, one can note that (i) if γ_1 and ω are fixed, the minimum distance between the manifolds (attained at the minimum of $h(m)$) increases by increasing the minimum of $h(m)$, the larger being the minimum of $h(m)$, the larger being the distance, and (ii) for a fixed ω, the larger is the minimum of $h(m)$, the larger is the multiplier $\gamma_{1,cr}$ needed to realize zero distance, namely the excitation amplitude for homoclinic bifurcation.

The previous observations are now put in a formal way. The general theory assures that, for ε sufficiently small, there is homoclinic intersection if and only if $\mathtt{M}(m)$ has a simple zero for some m, i.e., if and only if

$$h(m) = -\frac{\delta}{\gamma_1} \frac{\sinh(\omega\pi)}{5\pi\omega^2}, \tag{7}$$

for some m in $[0, 2\pi]$. Since the right hand side is a negative number, this is possible if and only if

$$\gamma_1 > \delta \frac{\sinh(\omega\pi)}{5\pi\omega^2} \frac{1}{M} \stackrel{\text{def}}{=} \gamma_{1,cr}(\omega), \tag{8}$$

where

$$M = -\min_{m\in[0,2\pi]} \{h(m)\} = \max_{m\in[0,2\pi]} \{-h(m)\} \tag{9}$$

is a positive number which depends on the shape but not on the amplitude γ_1 of the excitation.

In the special case of harmonic excitation, which is usually employed to analyze the basic nonlinear forced dynamics of a mechanical system and is therefore considered as a *reference* case to

measure the effectiveness of the method [13], one has $h(m) = \cos(m + \Psi_1)$, $M = 1$ and the corresponding critical curve $\gamma^h_{1,cr} = \delta \sinh(\omega\pi)/(5\pi\omega^2)$. Thus, the Melnikov's distance can be rewritten in the useful form

$$\mathtt{M}(m) = -\frac{6}{5}\delta\left[1 + \frac{\gamma_1}{\gamma^h_{1,cr}(\omega)}\,h(m)\right], \tag{10}$$

while the critical curve for a generic excitation is given by

$$\gamma_{1,cr}(\omega) = \frac{\gamma^h_{1,cr}(\omega)}{M}. \tag{11}$$

In the space of governing parameters (ω, γ_1), the curve $\gamma_{1,cr}(\omega)$ (corresponding to a generic excitation) separates the zone where homoclinic intersections do not occur (below the critical curve) from that where homoclinic intersections do occur (above the critical curve). The same holds for $\gamma^h_{1,cr}(\omega)$ in the case of harmonic excitation. These curves, which are depicted in Fig. 2, differ by a factor $1/M$ and they both tend to infinity for $\omega \to 0$ and for $\omega \to \infty$. There is only one minimum of the curve $\gamma_{1,cr}$ for $\omega_{res} = 0.6096$ and $\gamma_{1,cr} = 0.5688\delta/M$.

The central idea of the control method is to reduce the region of homoclinic intersection of Fig. 2 by varying the shape of the excitation. Since the dependence of $\gamma_{1,cr}$ on the shape is due only to the number M, the upper region is reduced when decreasing M, the smaller being M the smaller being the upper region in the parameter space. To quantitatively measure the improvement obtainable with respect to the reference harmonic excitation, the *gain* is introduced, which is defined as the ratio between the critical amplitudes of the unharmonic and harmonic excitations (see Eq. (11)),

$$G = \frac{\gamma_{1,cr}}{\gamma^h_{1,cr}} = \frac{1}{M}. \tag{12}$$

The zone where there is homoclinic intersection with harmonic excitation (above $\gamma^h_{1,cr}(\omega)$) and no intersection with unharmonic excitation (below $\gamma_{1,cr}(\omega)$) is the region where the control is expected to be effective, at least from a theoretical point of view, and it is called *saved region* (Fig. 2).

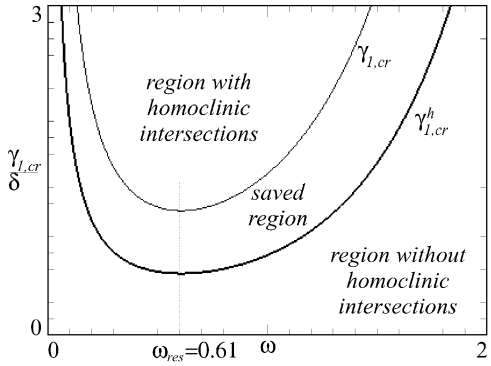

Fig. 2. The curves $\gamma^h_{1,cr}$ and $\gamma_{1,cr}$ for $M = 0.5$.

It is now clear that in order to enlarge the saved region as much as possible, one has to solve the following optimization problem:

$$\text{Maximizing } G \text{ by varying the Fourier coefficients } h_j \text{ and } \Psi_j,\ j = 2, 3, \ldots, \text{ of } h(m). \tag{13}$$

This problem, which arises also in the control of other systems, as shown in the following sections, will be analyzed in detail and solved in various forms in Section 3.1. After having determined the best h_j's and Ψ_j's, the Fourier coefficients γ_j can be computed by inverting relation (6b), and the optimal excitation is given by

$$\gamma(s) = \gamma_1 \sum_{j=1}^{\infty} h_j \frac{\sinh(j\omega\pi)}{j^2 \sinh(\omega\pi)} \sin(js + \Psi_j). \tag{14}$$

For the following purposes, it is worth emphasizing that, up to now, Eq. (13) is an abstract mathematical problem with no memory of the original mechanical system, which indeed enters only the Melnikov function, namely, when passing from the optimal solution $h(m)$ to the optimal excitation $\gamma(s)$ (Eq. (14)) using relations (6b).

2.1.2. Helmholtz–Duffing equation: the single-well potential with two asymmetric escape directions

A more realistic model of asymmetric ship rolling, entailing a more accurate (third instead of second order) approximation of the restoring hydrostatic potential [26] and allowing escape on both directions with a different level of dangerousness, is that described by the softening Helmholtz–Duffing equation. This is the particular case of Eq. (1) with $F(x) = \sigma x + (\sigma - 1)x^2 - x^3$ and can be written in the standard form

$$\ddot{x} + \varepsilon\delta\dot{x} + \sigma x + (\sigma - 1)x^2 - x^3 = \varepsilon\gamma(\omega t), \tag{15}$$

where σ is a parameter which measures the asymmetry of the system with respect to the unique rest position $x = 0$ and is assumed greater than 1 without loss of generality. For $\sigma \to 1$ one has the symmetric case, i.e., the standard softening Duffing oscillator (Section 2.1.3), while the other limit case $\sigma \to \infty$ leads, after rescaling, to the Helmholtz equation discussed in the previous section.

The potential $V(x) = \sigma x^2/2 + (\sigma - 1)x^3/3 - x^4/4$ for $\sigma = 1.5$ is depicted in Fig. 3a, which also shows how the escape is likely to occur in the negative direction, even if it is allowed for in the other direction, too, while the unperturbed phase space is depicted in Fig. 3b. As in the case of Section 2.1.1, the left escape from the potential well, triggered by the homoclinic bifurcation of the lower hilltop saddle, is the main—although not the unique—undesired phenomenon to be controlled by the proposed method.

Apart from the centre $x_2 = 0$, in the unperturbed undamped dynamics of Eq. (15) there are two saddles $x_1 = -1$ and $x_3 = \sigma$. Only the left (energetically lower) saddle $x_1 = -1$ has, on its right (see Fig. 3b), the homoclinic loop

$$x_{hom}(t) = -1 + \frac{3\sqrt{2}(\sigma + 1)}{\sqrt{(\sigma - 1)(2\sigma + 1)\cosh(t\sqrt{\sigma + 1}) + (\sigma + 2)\sqrt{2}}} \tag{16}$$

surrounding the unique potential well, while all the other invariant manifolds diverge to infinity.

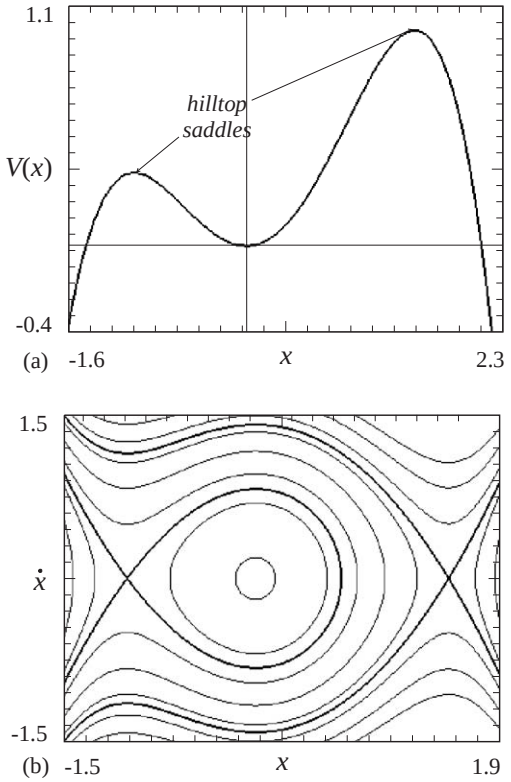

Fig. 3. (a) The potential $V(x)$ and (b) the unperturbed phase space of the softening Helmholtz–Duffing equation (15) for $\sigma = 1.5$.

The Melnikov's function is again formally given by Eq. (4), which in the present case leads to the more involved expression

$$\mathtt{M}(m) = -\frac{4}{9}\left[\delta f(\sigma) + \gamma_1 \frac{9\pi\omega}{\sqrt{2}} \frac{\sin\left[\dfrac{\omega}{\sqrt{\sigma+1}} \operatorname{arccosh}\left(\dfrac{(\sigma+2)\sqrt{2}}{\sqrt{(\sigma-1)(2\sigma+1)}}\right)\right]}{\sinh\left(\dfrac{\omega\pi}{\sqrt{\sigma+1}}\right)} h(m)\right], \tag{17}$$

where

$$f(\sigma) = \sqrt{\sigma+1}(\sigma^2+\sigma+1) - \frac{\sqrt{2}}{3}(\sigma+2)(2\sigma+1) \times (\sigma-1)\operatorname{arctanh}\sqrt{\frac{(\sigma+2)\sqrt{2} - \sqrt{(2\sigma+1)(\sigma-1)}}{(\sigma+2)\sqrt{2} + \sqrt{(2\sigma+1)(\sigma-1)}}}, \tag{18a}$$

$$h(m) = \sum_{j=1}^{\infty} h_j \cos(jm + \Psi_j), \tag{18b}$$

$$h_j = \frac{\gamma_j}{\gamma_1} j \frac{\sinh\left(\dfrac{\omega\pi}{\sqrt{\sigma+1}}\right)}{\sinh\left(\dfrac{j\omega\pi}{\sqrt{\sigma+1}}\right)} \frac{\sin\left[\dfrac{j\omega}{\sqrt{\sigma+1}}\operatorname{arccosh}\left(\dfrac{(\sigma+2)\sqrt{2}}{\sqrt{(\sigma-1)(2\sigma+1)}}\right)\right]}{\sin\left[\dfrac{\omega}{\sqrt{\sigma+1}}\operatorname{arccosh}\left(\dfrac{(\sigma+2)\sqrt{2}}{\sqrt{(\sigma-1)(2\sigma+1)}}\right)\right]}. \tag{18c}$$

Note once again that $h_1 = 1$ and that $h(m)$ is 2π-periodic and has zero mean value. The function $f(\sigma)$, which represents the contribution of the asymmetry to the constant part of the Melnikov's distance, is a strictly positive increasing function ranging from $f(1) = 3\sqrt{2}$ to $f(\infty) = \infty$.

The Melnikov function (17) resembles that of Section 2.1.1. However, there is a basic difference. In fact, while in Eq. (5) the amplitude of the oscillating part $h(m)$ is always positive, in the present case it oscillates with ω. More precisely, it is positive if

$$2k\pi \leqslant \frac{\omega}{\sqrt{\sigma+1}}\operatorname{arccosh}\left(\frac{(\sigma+2)\sqrt{2}}{\sqrt{(\sigma-1)(2\sigma+1)}}\right) \leqslant (2k+1)\pi, \quad k \in \mathbb{N} \tag{19}$$

and negative in the opposite case. In particular, for

$$\frac{\omega}{\sqrt{\sigma+1}}\operatorname{arccosh}\left(\frac{(\sigma+2)\sqrt{2}}{\sqrt{(\sigma-1)(2\sigma+1)}}\right) = k\pi, \quad k \in \mathbb{N}, \tag{20}$$

the oscillating part vanishes identically so that there is no homoclinic bifurcation for these "antiresonant" values of the excitation frequency.

The condition $\mathtt{M}(m) = 0$ for homoclinic bifurcation is expressed in the present case by

$$h(m) = -\frac{\delta}{\gamma_1}\frac{f(\sigma)\sqrt{2}}{9\pi\omega} \frac{\sinh\left(\dfrac{\omega\pi}{\sqrt{\sigma+1}}\right)}{\sin\left[\dfrac{\omega}{\sqrt{\sigma+1}}\operatorname{arccosh}\left(\dfrac{(\sigma+2)\sqrt{2}}{\sqrt{(\sigma-1)(2\sigma+1)}}\right)\right]}. \tag{21}$$

Contrary to Eq. (7), the right hand side is no longer positive for all the excitation frequencies, so that the two cases must be considered separately. When Eq. (19) holds, the right hand side of Eq. (21) is negative, and the homoclinic intersection is possible if and only if

$$\gamma_1 > \delta\frac{f(\sigma)\sqrt{2}}{9\pi\omega} \frac{\sinh\left(\dfrac{\omega\pi}{\sqrt{\sigma+1}}\right)}{\sin\left[\dfrac{\omega}{\sqrt{\sigma+1}}\operatorname{arccosh}\left(\dfrac{(\sigma+2)\sqrt{2}}{\sqrt{(\sigma-1)(2\sigma+1)}}\right)\right]}\frac{1}{M} \stackrel{\text{def}}{=} \gamma_{1,cr}, \tag{22}$$

where

$$M = -\min_{m\in[0,2\pi]}\{h(m)\} = \max_{m\in[0,2\pi]}\{-h(m)\} \tag{23}$$

is a positive number which accounts for the *shape* of the excitation. In the opposite case, the right hand side of Eq. (21) is positive, and the homoclinic intersection is possible if and only if

$$\gamma_1 > -\delta\frac{f(\sigma)\sqrt{2}}{9\pi\omega}\frac{\sinh\left(\dfrac{\omega\pi}{\sqrt{\sigma+1}}\right)}{\sin\left[\dfrac{\omega}{\sqrt{\sigma+1}}\operatorname{arccosh}\left(\dfrac{(\sigma+2)\sqrt{2}}{\sqrt{(\sigma-1)(2\sigma+1)}}\right)\right]}\frac{1}{M} \stackrel{\text{def}}{=} \gamma_{1,cr}, \tag{24}$$

where now the number M is given by

$$M = \max_{m\in[0,2\pi]}\{h(m)\}. \tag{25}$$

The curve $\gamma_{1,cr}(\omega,\sigma)$ is thus given by Eqs. (22)–(23) in intervals (19) and by Eqs. (24)–(25) elsewhere, and it is depicted in Fig. 4 for $\sigma = 1.01$, which should be compared with the previous Fig. 2. The overall shape of the curve is governed by the term $f(\sigma)\sqrt{2}\sinh(\omega\pi/\sqrt{\sigma+1})/(9\pi\omega)$ (the dotted envelope in Fig. 4), while the harmonic denominator is responsible for the "anti-resonant" values, which in the present case are given by $\omega = k1.1446,\ k\in\mathbb{N}$ (only the first is observable in Fig. 4). A Melnikov's curve similar to that reported in Fig. 4 has been previously observed, for example, by Yagasaki [27, Fig. 3] in the analysis of the hardening Duffing equation with parametric and external harmonic excitations.

In practice, the first U-shaped region of the diagram is the most important, as it entails the homoclinic bifurcation for the lowest value of the excitation. In the case of Fig. 4 the (lowest) chaotic resonance occurs for $\omega_{res} = 0.4777$ and $\gamma_{1,cr}(\omega_{res}) = 0.5785\delta/M$.

To obtain expressions similar to Eqs. (10)–(11), which highlight the common root of different mechanical systems with respect to the present control method, one observes that with harmonic

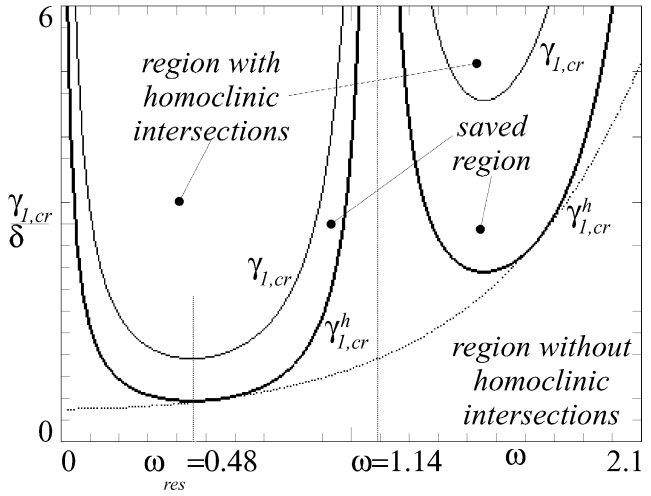

Fig. 4. The curves $\gamma^h_{1,cr}$ and $\gamma_{1,cr}$ for $M = 0.5$ and $\sigma = 1.01$.

excitation $M = 1$ for all ω's and the corresponding critical curve is denoted by $\gamma^h_{1,cr}$ (see Fig. 4), so that the Melnikov's distance can be rewritten in the common form

$$\mathtt{M}(m) = -\frac{4}{9}\delta f(\sigma)\left[1 \pm \frac{\gamma_1}{\gamma^h_{1,cr}(\omega)}h(m)\right], \tag{26}$$

where the sign plus is to be used in intervals (19) and the minus elsewhere. The critical curve $\gamma_{1,cr}(\omega,\sigma)$, on the other hand, can still be written in form (11), so that the gain is $G = 1/M$, but now the number M is defined by Eq. (23) in intervals (19) and by Eq. (25) elsewhere. Note that with the plus in Eq. (26) M is (minus) the minimum of $h(m)$, while with the minus it is the maximum of $h(m)$.

As in the Helmholtz oscillator, (i) the shape of the excitation modifies the critical value $\gamma_{1,cr}$ only by means of the number M, and the smaller is M the smaller is the region with homoclinic intersections; (ii) the zone where the unharmonic excitation is effective is called *saved region* in Fig. 4; (iii) in order to avoid homoclinic bifurcation, as much as possible, one has to solve the optimization problem (13); (iv) after having determined the best h_j's and Ψ_j's, the optimal excitation can finally be obtained by inverting relations (18c).

Remark 1. In addition to the previous similitudes, there is a single difference, resting on the different definition of M for different intervals of the excitation frequency. However, this difference is only formal and not substantial, because the associated optimization problems are in fact equivalent. With definition (23) one has to minimize the maximum of $-h(m)$, while with Eq. (25) one has to minimize the maximum of $+h(m)$. The solution of the latter problem is just the solution of the former with the even Fourier coefficients changed of sign or, equivalently, it is $-\bar{h}(m+\pi)$, where $\bar{h}(m)$ is the solution of the former problem. However, these solutions are different, although strictly related, so that the optimal excitation is step-wise dependent on the value of the excitation frequency.

2.1.3. Duffing equation: the single-well potential with two symmetric escape directions

In rolling of symmetric cargo in a symmetric environment [28], the capsize is allowed to occur both on the right and on the left directions, and the restoring hydrostatic potential has symmetric barriers with respect to the rest position. This case is described by the symmetric version of Eq. (15), which is obtained by choosing $\sigma = 1$

$$\ddot{x} + \varepsilon\delta\dot{x} + x - x^3 = \varepsilon\gamma(\omega t) \tag{27}$$

(note that a different scaling is used with respect to Ref. [28], that the quadratic viscous damping is neglected and that water-on-deck is excluded). Eq. (27) describes the single mode dynamics of other mechanical systems and structures, and it is an archetype for the dynamics of a class of 1-d.o.f. mechanical systems (see, for example, Refs. [29,30]), in particular, for those which are just below a non-degenerate subcritical pitchfork bifurcation.

Contrary to Eq. (15), the capsizing (escape from the potential well) is equally probable in both directions, because the two hilltop saddles $x_{3,1} = \pm 1$ have the same energy level. This property in turn implies that the homoclinic loop of Eq. (15) is substituted by a heteroclinic loop, with the two

heteroclinic orbits given by

$$x_{het}(t) = \pm\tanh(t/\sqrt{2}). \tag{28}$$

On each heteroclinic orbit, the Melnikov function is given by Eq. (4) with $x_{het}(t)$ instead of $x_{hom}(t)$ [10], and after some computations this yields

$$\mathtt{M}(m) = -\delta\frac{2\sqrt{2}}{3}\left[1 \mp \frac{\gamma_1}{\gamma^h_{1,cr}(\omega)}h(m)\right], \tag{29}$$

where

$$\gamma^h_{1,cr}(\omega) = \delta\frac{2}{3}\frac{\sinh\left(\dfrac{\omega\pi}{\sqrt{2}}\right)}{\omega\pi}, \qquad h(m) = \textstyle\sum_{j=1}^{\infty} h_j \sin(jm + \Psi_j),$$
$$h_j = \frac{\gamma_j}{\gamma_1}\frac{j\sinh\left(\dfrac{\omega\pi}{\sqrt{2}}\right)}{\sinh\left(\dfrac{j\omega\pi}{\sqrt{2}}\right)}. \tag{30a–c}$$

The heteroclinic bifurcation under generic excitation occurs for $\gamma_{1,cr} = \gamma^h_{1,cr}/M$, where $M = \max\{h(m)\}$ for the orbit going from -1 to $+1$ (sign minus in Eq. (29)) and $M = -\min\{h(m)\}$ for the other orbit (sign plus in Eq. (29)).

If the amplitude threshold of only one of the two heteroclinic bifurcations is to be increased, *irrespective* of what happens to the other, the optimization problem (13) with the appropriate choice of $G = 1/M$ must be solved, and this basically leads to the same mathematical problem, as noted in Remark 1. This strategy permits to break the (perturbed) heteroclinic loop responsible for the chaotic saddle via the horseshoe dynamics, and therefore it contributes to regularize the non-linear dynamics of the system, to eliminate part of the fractal basin boundaries and to reduce unpredictability. However, the heteroclinic intersection of the non-controlled orbit allows for the penetration of tongues of the basin of attraction of the infinity into the basins of the finite attractors (usually defined as *safe basin* [11]), and this may result in a faster safe basin erosion leading to an earlier failure of the system. Thus, a different strategy, aimed at preserving the lifetime of the system, may be that of avoiding *simultaneously* the upper and lower heteroclinic bifurcations.

The simultaneous shift of the two bifurcations entails the simultaneous decrement of $-\min\{h(m)\}$ and of $\max\{h(m)\}$. It is possible to numerically show (see Section 3.2) that the optimal solution is characterized by the condition $-\min\{h(m)\} = \max\{h(m)\}$, so that in the present case the optimization problem is

$$\text{Maximizing } G \text{ by varying the Fourier coefficients } h_j \text{ and}$$
$$\Psi_j,\ j = 2, 3, \ldots, \text{ of } h(m), \text{ under the constraint} - \min\{h(m)\} = \max\{h(m)\}, \tag{31}$$

where, due to the constraint, there is no ambiguity in the definition of the gain. This problem is just problem (13) with the addition of the constraint accounting for the simultaneous control of

the two heteroclinic bifurcations. It will be encountered in a similar context in the following (see Section 2.2), and will be analyzed in detail and solved in various forms in Section 3.2.

2.1.4. The mathematical pendulum

Another largely investigated dynamical system is the mathematical pendulum, which stands as one of the most important archetype for the analysis of various aspects of non-linear dynamics [8,10,31]. It is governed by the equation

$$\ddot{x} + \varepsilon\delta\dot{x} + \sin(x) = \varepsilon\gamma(\omega t), \tag{32}$$

obtained by posing $F(x) = \sin(x)$ in Eq. (1).

It falls in the realm of the present work, and its analysis is qualitatively identical to that of Section 2.1.3, because, after rescaling, Eq. (27) is just the third order approximation of Eq. (32). Accordingly, only the expressions of the heteroclinic orbits, of the Melnikov function and of the critical curve for the harmonic excitation are reported:

$$x_{het}(t) = \pm 2\mathrm{atan}[\sinh(t)], \tag{33a}$$

$$\mathtt{M}(m) = -8\delta\left[1 \mp \frac{\gamma_1}{\gamma^h_{1,cr}(\omega)} h(m)\right], \tag{33b}$$

$$\gamma^h_{1,cr}(\omega) = \delta\frac{4}{\pi}\cosh\left(\frac{\omega\pi}{2}\right), \qquad h(m) = \textstyle\sum_{j=1}^{\infty} h_j \sin(jm + \Psi_j),$$

$$h_j = \frac{\gamma_j}{\gamma_1}\frac{\cosh(\omega\pi/2)}{\cosh(j\omega\pi/2)}. \tag{33c–e}$$

2.2. Hardening oscillators

In this paper only the class of two-well hardening oscillators, representing the most common mechanical systems, will be considered. The case of several potential wells, which deserves a theoretical interest but is concerned only with specific applications, will be discussed in the future. In this section *symmetric* oscillators are considered, whereas a representative case of *asymmetric* oscillator is considered in Ref. [23].

2.2.1. Duffing equation: symmetric two-well potential

The hardening twin-well Duffing equation is one of the most widely investigated equations in the field of applied non-linear dynamics [1,3,8,10] and it describes the single-mode non-linear dynamics of buckled beams [32], of magnetoelastic pendulum [3] and of many others mechanical systems and structures. It can be written in the form

$$\ddot{x} + \varepsilon\delta\dot{x} - x + 2x^3 = \varepsilon\gamma(\omega t), \tag{34}$$

which is the particular case of Eq. (1) with $F(x) = -x + 2x^3$. The associated potential $V(x) = -x^2/2 + x^4/2$ and the unperturbed phase space are depicted in Figs. 5a and b, respectively.

In addition to the previous mechanical applications, Eq. (34) is the archetype of twin-well symmetric oscillators and exhibits very rich non-linear dynamics. For example, for large values of the excitation there is a cross-well (scattered) chaotic attractor, which substitutes the escape to

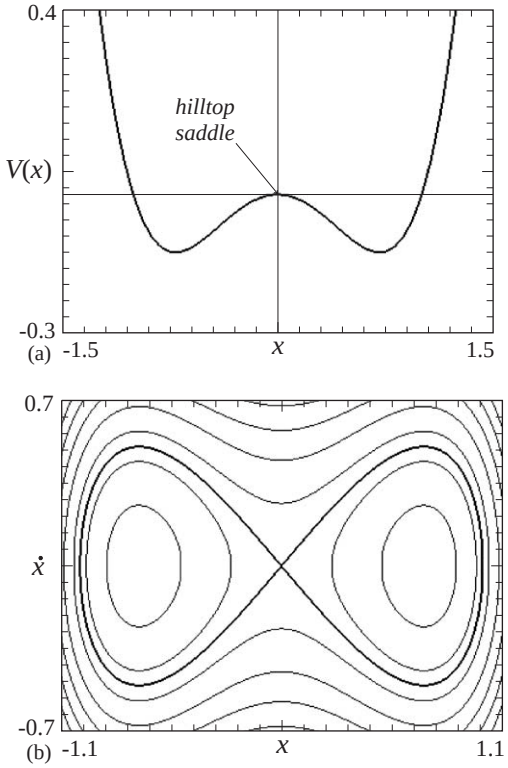

Fig. 5. (a) The potential $V(x)$ and (b) the unperturbed phase space of the hardening Duffing equation (34).

infinity of the previous softening oscillators [25,33], and is considered as one of the unwanted dynamical events whose elimination (or shift) represents a very desirable practical performance of the control method [34].

The unperturbed undamped dynamics are characterized by the presence of two centres x_1 and x_3 and a unique (hilltop) saddle $x_2 = 0$, now having *two* symmetric homoclinic loops, one on the right and one on the left of the phase space (see Fig. 5b), which can be expressed in the following form:

$$x_{hom}^{r,l}(t) = \pm\frac{1}{\cosh(t)}. \tag{35}$$

The presence of two simultaneous homoclinic orbits, apparently analogous to the heteroclinic ones of Sections 2.1.3 and 2.1.4, is the new point with respect to the cases of Sections 2.1.1 and 2.1.2, and it has very important consequences in terms of control, as will be shown in the following. Accordingly, there are two different Melnikov's functions, formally given by Eq. (4), which can be written in the standard form

$$\mathrm{M}^{r,l}(m) = -\delta\frac{2}{3}\left[1 \pm \frac{\gamma_1}{\gamma_{1,cr}^{h}(\omega)}h(m)\right], \tag{36a}$$

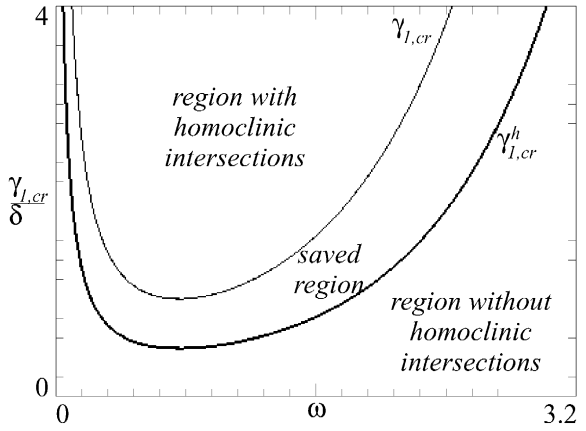

Fig. 6. The curves $\gamma^h_{1,cr}$ and $\gamma_{1,cr}$ for $M = 0.5$.

$$\gamma^h_{1,cr}(\omega) = \delta \frac{2}{3\pi\omega} \cosh\left(\frac{\omega\pi}{2}\right) > 0, \tag{36b}$$

$$h(m) = \sum_{j=1}^{\infty} h_j \cos(jm + \Psi_j), \qquad h_j = \frac{\gamma_j}{\gamma_1} j \frac{\cosh\left(\frac{\omega\pi}{2}\right)}{\cosh\left(\frac{j\omega\pi}{2}\right)}. \tag{36c, d}$$

The curve $\gamma^h_{1,cr}(\omega)$ represents the loci of the right *and* left homoclinic bifurcations (they coincide) in the reference case of harmonic excitation, and is depicted in Fig. 6.

The peculiarity of the present oscillator appears at this point. In fact, the presence of two homoclinic orbits permits to choose among different control strategies. Indeed, one can control *only* the right (left) homoclinic bifurcation, irrespective of what happens in the left (right) potential well, or one can try to control *simultaneously* the right and the left homoclinic bifurcations. This question, anticipated in Section 2.1.3 with reference to the heteroclinic bifurcations, becomes herein more important from the application viewpoint, since the first approach is aimed at obtaining a topologically "localized" control, whereas the second approach is aimed at controlling, on average, the "whole" phase space. The two approaches have been discussed in detail by the authors in the case of the inverted pendulum [18,35], where it has been shown that the former ("one-side" control) provides large gains, while the latter ("global" control) provides lower gains. Their different features have been shown in Ref. [18], where it is also numerically confirmed that, at least for the inverted pendulum, the global and one-side controls are actually complementary rather than competing.

The three different cases are now investigated separately:

(ia) "*One-side*" *control on the right well* (*right control*): The condition $\mathtt{M}^r(m) = 0$ for some $m \in [0, 2\pi]$, guaranteeing the homoclinic intersection of the right stable and unstable manifolds, occurs in the region of the parameter space defined by

$$\gamma_1 > \gamma^r_{1,cr} = \gamma^h_{1,cr} \frac{1}{M^r}, \tag{37}$$

where, as in Eq. (23),

$$M^r = -\min_{m\in[0,2\pi]}\{h(m)\} = \max_{m\in[0,2\pi]}\{-h(m)\} \tag{38}$$

is a positive number which accounts for the *shape* of the excitation. To avoid right homoclinic tangency by an appropriate choice of the shape of the excitation, the gain $G =^{\text{def}} G^r = 1/M^r$ must be maximized, i.e., problem (13) must be solved, and then the optimal excitation is obtained by way of Eq. (36d).

(ib) "*One-side*" *control on the left well* (*left control*): The condition $\mathtt{M}^l(m) = 0$ for some $m\in[0,2\pi]$, guaranteeing the homoclinic intersection of the left stable and unstable manifolds, occurs in the region of the parameter space defined by

$$\gamma_1 > \gamma^l_{1,cr} = \gamma^h_{1,cr}\frac{1}{M^l}, \tag{39}$$

where, as in Eq. (25),

$$M^l = \max_{m\in[0,2\pi]}\{h(m)\} \tag{40}$$

is a positive number which accounts for the *shape* of the excitation. To avoid left homoclinic tangency by an appropriate choice of the shape of the excitation, the gain $G =^{\text{def}} G^l = 1/M^l$ must be maximized, i.e., problem (13) must be solved, and then the optimal excitation is obtained by way of Eq. (36d). Actually, the optimal gains obtainable with the two one-side controls are equal, see Remark 1.

(ii) "*Global*" *control*: To control *simultaneously* the right and the left homoclinic tangencies, the right and the left gains, $G^r = 1/M^r$ and $G^l = 1/M^l$, where $M^r = -\min\{h(m)\}$ and $M^l = \max\{h(m)\}$, must be increased simultaneously.

Mathematically, increasing G^r and G^l simultaneously entails increase of their minimum value, namely

$$\begin{gathered}\text{Maximizing } G = \min\{G^r, G^l\} \text{ by varying the coefficients } h_j \text{ and}\\ \Psi_j,\ j = 2,3,\ldots, \text{ of } h(m).\end{gathered} \tag{41}$$

However, all the numerical solutions of Eq. (41) which will be obtained in Section 3.2 will satisfy the condition $G^r = G^l =^{\text{def}} G$ as expected, namely, $-\min\{h(m)\} = \max\{h(m)\}$. In such a case, problem (41) can be rewritten in the simplified form (31), which shows that Eq. (41) is actually a constrained version of Eq. (13). Accordingly, the optimal gain is lesser than that of Eq. (13), as it will be confirmed numerically in Section 3.2. The counterpart of this reduction is the possibility to control the whole phase space.

2.2.2. Non-linear equation with large odd stiffness

For illustrative purposes, in the previous section the control method has been developed with reference to the classical Duffing equation with cubic non-linearity, which permits easy computations. However, this is a particular case of the more general class of oscillators with odd non-linearities

$$\ddot{x} + \varepsilon\delta\dot{x} - x + nx^{2n-1} = \varepsilon\gamma(\omega t), \tag{42}$$

which are obtained by choosing $F(x) = -x + nx^{2n-1}$ in Eq. (1) ($n \in \mathbb{N}, n > 1$) and can be treated analogously. The associated potential is $V(x) = -x^2/2 + x^{2n}/2$ which, compared with that of Fig. 5, is much sharper for $|x| > 1$.

The present case is formally identical to that of Section 2.2.1, and the same control strategies apply. Accordingly, only the expressions of the homoclinic orbits, of the Melnikov function and of the critical curve for the harmonic excitation are reported

$$x_{hom}^{r,l}(t) = \pm \frac{1}{\cosh^{1/(n-1)}[(n-1)t]}, \tag{43a}$$

$$\mathtt{M}^{r,l}(m) = -\delta f(n)\left[1 \pm \frac{\gamma_1}{\gamma_{1,cr}^{h}(\omega)}\, h(m)\right], \tag{43b}$$

$$\gamma_{1,cr}^{h}(\omega) = \delta \frac{f(n)}{g(\omega, n)} > 0, \tag{43c}$$

$$h(m) = \sum_{j=1}^{\infty} h_j \cos(jm + \Psi_j), \qquad h_j = \frac{\gamma_j}{\gamma_1} \frac{g(j\omega, n)}{g(\omega, n)}, \tag{43d, e}$$

where ($\Gamma(z) = \int_0^\infty t^{z-1} \mathrm{e}^{-t}\, \mathrm{d}t$ is the gamma function [36])

$$f(n) = \frac{n 4^{n/(n-1)}}{\Gamma\left(\dfrac{2n}{n-1}\right)} \sum_{k=0}^{\infty} (-1)^k \frac{\Gamma\left(k + \dfrac{2n}{n-1}\right)}{k![n + k(n-1)]} - \frac{4^{1/(n-1)}}{\Gamma\left(\dfrac{2}{n-1}\right)} \sum_{k=0}^{\infty} (-1)^k \frac{\Gamma\left(k + \dfrac{2}{n-1}\right)}{k![1 + k(n-1)]}, \tag{44a}$$

$$g(\alpha, n) = \frac{2^{n/(n-1)}}{\Gamma\left(\dfrac{1}{n-1}\right)} \sum_{k=0}^{\infty} (-1)^k \frac{\Gamma\left(k + \dfrac{1}{n-1}\right)}{\Gamma(k+1)} \frac{1}{\dfrac{\alpha}{2k(n-1)+1} + \dfrac{2k(n-1)+1}{\alpha}}. \tag{44b}$$

Eqs. (43) and (44) reduce to the corresponding ones of Section 2.2.1 in the case of classical Duffing equation $n = 2$ (in fact, $f(2) = 2/3$ and $g(\alpha, 2) = (\pi\alpha)/\cosh(\pi\alpha/2)$).

Remark 2. In the previous sections the various oscillators have been classified with respect to their main mechanical properties, in particular, the kind of stiffness (hardening/softening), which permits a clear distinction between the physical undesired phenomena one wishes to control. In fact, while for softening oscillators the drawback is the erosion of the safe basin [12] and the successive escape from the potential well, for hardening systems it is the cross-well steady chaos. However, it is also possible to pursue another classification of the considered oscillators, based on their symmetric or asymmetric nature. This distinction deserves attention from a dynamical

systems point of view, because, apart from some pathological situations, symmetric oscillators are structurally unstable and are particular cases of asymmetric oscillators, though not always being a limit, in an appropriate sense, of the latter, as shown by the case of the softening (Helmholtz–) Duffing equation.

3. Optimal problems and solutions

In Section 2 it has been shown how the problems of avoiding homoclinic or heteroclinic intersections can be mathematically formulated as appropriate optimization problems. Moreover, it has been shown that there is only one basic mathematical *problem* of optimization (Eq. (13)) where the minimum (or the maximum) of $h(m)$ is controlled (one-side controls), with an added constraint in the case of global control (Eq. (31)). This ensues from the basic role played by the homo/heteroclinic connection of proper hilltop saddles in the system phase space organization and evolution, which is a common aspect to the *non-linear dynamics* of various mechanical systems. It also entails a common character of the problem *solution*, because problems (13) and (31) are system independent and can be solved without any reference to the specific oscillator. They will be addressed in Sections 3.1 and 3.2, respectively.

In previous works of the authors [17,18], the control method has been applied to a symmetric inverted pendulum with unilateral barriers, whose dynamics are non-smooth due to the impacts on the lateral walls. The analysis is simpler, thanks to the hypothesis of piece-wise linearity, and it does not require the Melnikov theory because the distance between stable and unstable manifolds can be computed exactly. This system leads just to the optimization problems (13) and (31) in the case of one-side and global control, respectively, the only difference being in the relation between the excitation and $h(m)$. This fact further supports the *generic* character of the two optimization problems (13) and (31) and of their solutions, which actually hold in the case of non-smooth dynamics, too; generally speaking, this underlines the generic character of the control.

3.1. One-side control

When only one homoclinic bifurcation is to be controlled, the associated optimization problem is Eq. (13), which is rewritten in a form more appropriate for computing its solution:

$$\begin{gathered}\text{Maximizing } \min_{m\in[0,2\pi]}\{h(m)\} \text{ by varying the Fourier coefficients } h_j \\ \text{and } \Psi_j,\ j=2,3,\ldots, \text{ of } h(m)=\cos(m+\psi_1)+\sum_{j=2}^{\infty} h_j\cos(jm+\Psi_j).\end{gathered} \tag{45}$$

The gain associated to the previous problem, which measures the effectiveness of the optimal solution with respect to the harmonic case, is $G=-1/\min\{h(m)\}$, and the optimal gain is clearly the maximum of this expression.

Apart from inessential technical points, problem (45) is exactly the same mathematical problem which arises in the optimal chaos control of the inverted pendulum, which has been investigated in Ref. [17]. It has also been deeply studied and solved in various forms in Section 3 of Ref. [13], so that only the main points of that analysis and the necessary modifications required to extend its generality are summarized in the following.

3.1.1. Optimal solution

The solution $h(m)$ is given by a positive Dirac delta of amplitude π at $m = 0$ plus the constant function $-1/2$ [17]. The Fourier coefficients are $h_j = 1, \Psi_j = \Psi_1$ ($= 0$ without loss of generality) and the optimal gain is 2, i.e., the critical amplitude is doubled in principle.

Unfortunately, the previous mathematical optimal solution is not acceptable from a physical point of view, because the corresponding optimal excitations would be a divergent series, as shown for example in the case of Section 2.1.1, whose optimal excitation would be (see Eq. (14))

$$\gamma(s) = \gamma_1 \sum_{j=1}^{\infty} \frac{\sinh(j\omega\pi)}{j^2 \sinh(\omega\pi)} \sin(js). \tag{46}$$

This drawback is not a pathological property of the Helmholtz oscillator, but holds in general. In fact, it is a consequence of the asymptotic relation ($P(j)$ is a polynomial expression in the j variable)

$$\gamma_j \cong h_j \ const.\mathrm{e}^{j\omega c}/P(j), \quad c > 0, \ j \to \infty, \tag{47}$$

between the Fourier coefficients of the $h(m)$ and of the excitation, which is shared by all the considered oscillators (see Eqs. (6b), (18c), (30c), (33e), (36d), (43e)).

The previous considerations mean that some further constraints should be added to problem (45) in order to take into account the physical admissibility of the searched optimal excitation. This will be done in different manners in the following sections. In any case, due to the new constraint, the physically admissible best gain is reduced, and the value $G = 2$ remains as a (hypothetically optimal) value of comparison (indeed, it is an upper bound) for the actual optimal problems: the more the constrained optimal G is close to 2, the more the associated optimal excitation is effective, at least from a theoretical point of view.

3.1.2. Optimal solutions with a finite number of superharmonics

The first way to obtain optimal admissible excitations is to consider only a finite number of superharmonic corrections added to the basic harmonic excitations, so that the question of convergence automatically disappears. Although it may appear unpleasant to give up the possibility of having infinite superharmonics, it will be shown in the following (see Table 1) that it is possible to obtain reduced-order solutions which are very satisfactory from a practical point of view, having a high gain and being easily reproducible in experiments and/or applications.

Initially, note that the choice $\Psi_j = \Psi_1 (= 0)$ remains optimal also with a finite number of superharmonics, so that the reduced optimal problems have actually the only variables h_j, $j = 2, 3, \ldots, N$. Furthermore, it is easy to verify that the functional to be maximized (which is the minimum of $h(m)$) is concave with respect to the variables h_j, and that the solution is unique.

The first case $N = 2$ corresponds to a single superharmonic, and can be solved analytically [13]. Easy computations show that the solution is $h(m) = \cos(m) + (\sqrt{2}/4)\cos(2m)$ corresponding to the optimal gain $G = \sqrt{2}$. Comparing this value with the upper bound $G = 2$, it is possible to see that, although the critical amplitude is considerably increased with respect to the harmonic excitation ($G = 1$) even with a single superharmonic, the upper bound is yet far, and better results can be obtained by adding further superharmonics. The corresponding optimal problems are, however, more difficult and are solved numerically.

Table 1
The numerical results of various optimization problems with increasing finite number of superharmonics in the case of one-side control

N	G_N	h_2	h_3	h_4	h_5	h_6	h_7	h_8	h_9
2	1.4142	0.353553							
3	1.6180	0.552756	0.170789						
4	1.7321	0.673525	0.333274	0.096175					
5	1.8019	0.751654	0.462136	0.215156	0.059632				
6	1.8476	0.807624	0.567084	0.334898	0.153043	0.042422			
7	1.8794	0.842528	0.635867	0.422667	0.237873	0.103775	0.027323		
8	1.9000	0.872790	0.706011	0.527198	0.355109	0.205035	0.091669	0.024474	
9	1.9130	0.877014	0.705931	0.518632	0.341954	0.195616	0.091497	0.031316	0.005929
∞	2	1	1	1	1	1	1	1	1

A MonteCarlo simulation with at least 50 000 trials is initially performed to localize the solution, and successively the method of Nelder and Mead [37] is adopted with reflection coefficient $\alpha = 1$, contraction coefficient $\beta = 0.9$ and expansion coefficient $\gamma = 1.1$ and with random initial condition. The numerical results are reported in Table 1, where the last row corresponds to the (non-admissible) case of Section 3.1.1 and is reported for the sake of comparison. It is clear from Table 1 that the optimal solutions with a finite number of superharmonics tend to the "mathematical" optimal solution of Section 3.1.1 when $N \to \infty$.

The results of Table 1 can be applied to any considered system (in this sense the solution to problem (45) could be referred to as "universal"). To illustrate this point, the external excitations of some mechanical systems considered in Section 2 in the case $N = 2$ are reported:

$$\gamma(s) = \gamma_1[\sin(s) + (\sqrt{2}/8)\cosh(\omega\pi)\sin(2s)], \quad \text{Helmholtz oscillator,} \tag{48a}$$

$$\gamma(s) = \gamma_1\left[\sin(s) + \frac{\sqrt{2}}{8}\frac{\cosh\left(\dfrac{\omega\pi}{\sqrt{\sigma+1}}\right)}{\cos\left[\dfrac{\omega}{\sqrt{\sigma+1}}\operatorname{arccosh}\left(\dfrac{(\sigma+2)\sqrt{2}}{\sqrt{(\sigma-1)(2\sigma+1)}}\right)\right]}\sin(2s)\right], \tag{48b}$$

softening Helmholtz–Duffing, ω satisfying Eq. (19),

$$\gamma^{lower}(s) = \gamma_1\left[\sin(s) + \frac{\sqrt{2}}{4}\cosh\left(\frac{\omega\pi}{\sqrt{2}}\right)\sin(2s)\right], \quad \text{softening Duffing,} \tag{48c}$$

$$\gamma^{r}(s) = \gamma_1\left[\sin(s) + \frac{\sqrt{2}\ \cosh(\omega\pi)}{8\ \cosh(\omega\pi/2)}\sin(2s)\right], \quad \text{hardening Duffing.} \tag{48d}$$

3.1.3. On the constrained problem with infinite number of superharmonics

The solutions obtained in the previous section are optimal within the restricted class of excitations with a finite number of superharmonics. Although they give gains which can be very

satisfactory for applications (see Table 1), they do not exploit the full potential of having *infinite* number of superharmonics, which is one important characteristic of the proposed control method. This point is addressed in this section.

It is worth while to initially emphasize that the loss of convergence is due to relation (47), which implies an exponential growth of the Fourier coefficients of the excitation. Among various possible choices for overcoming this point, only the bounds

$$|h_j| \leqslant A a^j, \quad j = 2, 3, \ldots, a < 1 \tag{49}$$

are considered in this section. In Eq. (49) A is a given constant related to the physical "cost" of the control, while the positive number a is of the form $a = \mathrm{e}^{-\omega c}$ and depends on the system. For example, for the Helmholtz equation $a = \mathrm{e}^{-\omega\pi}$, for the symmetric hardening Duffing equation $a = \mathrm{e}^{-\omega\pi/2}$, etc.

Inequalities (49) guarantee that

$$\begin{aligned} h(m) &= \cos(m + \psi_1) + \textstyle\sum_{j=2}^{\infty} h_j \cos(jm + \Psi_j) \leqslant \cos(m + \psi_1) + A \sum_{j=2}^{\infty} a^j \\ &= \cos(m + \psi_1) + A \frac{a^2}{1 - a}, \end{aligned} \tag{50}$$

so that

$$\min_{m \in [0, 2\pi]} \{h(m)\} \leqslant -1 + A \frac{a^2}{1 - a}, \tag{51}$$

or, remembering that $G = -1/\min\{h(m)\}$,

$$G \leqslant \frac{1}{1 - Aa^2/(1 - a)}, \tag{52}$$

which shows that the right-hand side is a (constrained) upper bound for the optimal gain G. Summing up Eq. (52) with the unconstrained upper bound $G \leqslant 2$, it is possible to obtain the following overall upper bound for the optimal gain:

$$G \leqslant \begin{cases} 2 & \text{if } A > \dfrac{1 - a}{a^2} \dfrac{1}{2}, \\ \dfrac{1}{1 - \dfrac{Aa^2}{(1 - a)}} & \text{if } A < \dfrac{1 - a}{a^2} \dfrac{1}{2}, \end{cases} \tag{53}$$

which is illustrated in Fig. 7 for various values of A. Inverting the lower right inequality in Eq. (53) one gets $a < (-1 + \sqrt{1 + 8A})/(4A)$, which shows that the constrained upper bound reduces the unconstrained upper bound $G \leqslant 2$ only for medium and low values of a, namely, remembering that $a = \mathrm{e}^{-\omega c}$, for medium and large values of ω. Actually, in this range the exact solution can be determined.

The test function [36, Eq. (17.17.2)]

$$h(m) = cos(m) + A \sum_{j=2}^{\infty} (-a)^j \cos(jm) = \cos(m) + Aa^2 \frac{\cos(2m) + a\cos(m)}{1 + 2a\cos(m) + a^2} \tag{54}$$

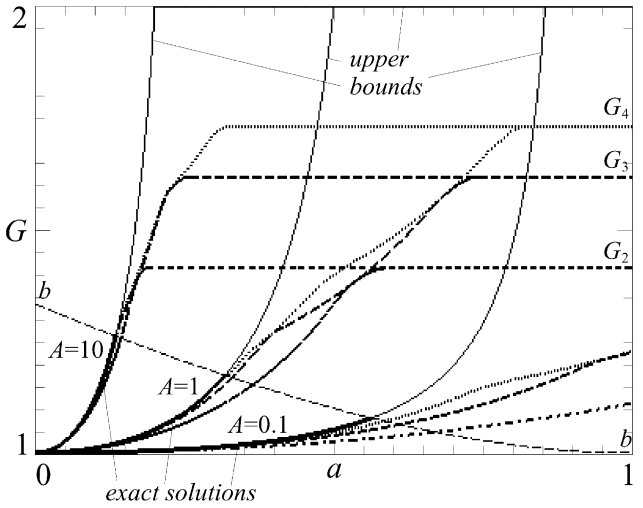

Fig. 7. The upper bound (53) of the optimal gain G for various values of A. The solid thick lines are the exact solutions of Proposition 1, while the line b–b delimits the range of validity of the exact solutions, and is given by Eq. (57). The other thick lines are the reduced (constrained and unconstrained) optimal gains G_2, G_3 and G_4, respectively.

satisfies constraints (49). It is possible to show that, for

$$A \leqslant \frac{(1-a)^3}{a^2(a^2-3a+4)}, \tag{55}$$

the minimum (attained for $m = \pi$) is $-1 + Aa^2/(1-a)$, and the associated gain is

$$G = \frac{1}{1 - Aa^2/(1-a)}. \tag{56}$$

Comparing Eq. (56) with Eq. (53) it is possible to see that the gain associated with the test function (54) coincides with the constrained upper bound, and this proves the following proposition:

Proposition 1. *In range* (55), *function* (54) *is a solution of problem* (45) *under constraint* (49).

The optimal gains (56) associated with the solution of Proposition 1 are depicted with solid lines in Fig. 7 for various values of A. The line b–b, on the other hand, delimits the range of validity of the exact solutions, and is obtained by substituting the limit value of A, given by Eq. (55) with the equality sign, in Eq. (56), thus providing the limiting value of the exact G

$$\frac{a^2-3a+4}{3-a}. \tag{57}$$

3.1.4. On the constrained problems with finite but bounded number of superharmonics

In this section the optimal problems with finite number of superharmonics, as those of Section 3.1.2, are considered under the assumption of the previous section that the

superharmonic corrections satisfy constraints (49). This is not required for convergence problems, as in Section 3.1.3, but it has rather different motivations. From one side, in fact, the results of the previous section do not provide any information on the constrained gain for high values of a, i.e., for low values of the excitation frequency (Fig. 7), where Proposition 1 does not apply. From the other side, the *feasibility* of the reduced optimal control of Section 3.1.2 should be improved. In fact, the optimal excitations may have very large superharmonic amplitudes for high but also for medium values of ω, as shown by Eq. (48), thus becoming practically useless. Accordingly, it is necessary to look for reduced optimal solutions with bounded amplitudes of the superharmonic corrections.

The reduced optimal solution with N terms satisfies constraints (49) as long as

$$a \geqslant |h_j/A|^{(1/j)}, \quad j = 2, 3, \ldots, N, \tag{58}$$

where the h_j are reported in Table 1.

As in Section 3.1.2, the first case $N = 2$ is the easier one and can be solved analytically. One has $G_2 = \sqrt{2}$ and $h_2 = \sqrt{2}/4$ for $1/(2^{(3/4)}A^{(1/2)}) < a$, $G_2 = 8Aa^2/(1 + 8A^2a^4)$ and $h_2 = Aa^2$ for $1/(2A^{(1/2)}) < a < 1/(2^{(3/4)}A^{(1/2)})$, $G_2 = 1/(1 - Aa^2)$ and $h_2 = Aa^2$ for $a < 1/(2A^{(1/2)})$. The curve $G_2 = G_2(a)$ is reported in Fig. 7 for various values of A.

The other cases $N > 2$ have been solved numerically with the same method as in Section 3.1.2, by accounting for constraints (49) through a penalty term added to the functional, and the resulting functions $G_N = G_N(a)$ are also reported in Fig. 7. Note how for increasing number of superharmonics the curves accumulate quite fast on a corresponding curve (for each given A value) which represents the optimal solution of the constrained optimal problem with infinite superharmonics.

3.2. Global control of two-well symmetric systems

In the case of global control of symmetric systems, the mathematical problem providing the optimal excitation is Eq. (31), which is rewritten in a form equivalent to Eq. (45) but differing from it for the presence of the constraint:

$$\begin{gathered}\text{Maximizing } \min_{m\in[0,2\pi]} \{h(m)\} \text{ by varying the Fourier} \\ \text{coefficients } h_j \text{ and } \Psi_j,\ j = 2, 3, \ldots, \text{ of } h(m) = \cos(m + \psi_1) + \sum_{j=2}^{\infty} h_j \cos(jm + \Psi_j), \\ \text{under the constraint } \min_{m\in[0,2\pi]} \{h(m)\} = -\max_{m\in[0,2\pi]} \{h(m)\}.\end{gathered} \tag{59}$$

3.2.1. Optimal solution

As for the case of one-side control, also the previous problem has been solved in Ref. [17]. The solution is the piecewise constant function

$$h(m) = \begin{cases} \dfrac{\pi}{4}, & 0 < m < \dfrac{\pi}{2},\ \dfrac{3\pi}{2} < m < 2\pi, \\ -\dfrac{\pi}{4}, & \dfrac{\pi}{2} < m < \dfrac{3\pi}{2}, \end{cases} \tag{60}$$

whose Fourier series, which has only odd superharmonics, is

$$h(m) = \sum_{j=1}^{\infty} \frac{1}{j} \sin\left(\frac{j\pi}{2}\right) \cos(jm), \tag{61}$$

and the optimal gain is $G = 4/\pi \cong 1.2732$. Thus, the theoretical optimal gain is drastically reduced with respect to the one-side control ($G = 2$), and this drawback counterbalances the advantage of controlling the whole phase space rather than only one part of it. This shows that the two approaches are actually complementary rather than competing, as noted in other authors' works [18], having complementary scopes and different theoretical gains.

The similitude with the one-side control is unhappily maintained also in the physical inadmissibility of the theoretical optimal solution (60), again due to Eq. (47), so that also in this case one must consider reduced, constrained and reduced/constrained optimal excitations, just as in Section 3.1. The value $G = 4/\pi$ is a theoretical upper bound and a term of comparison for the physically admissible solutions obtained in the following sections.

3.2.2. Optimal solutions with a finite number of superharmonics

The optimal solutions of problem (59) with increasing finite number of superharmonics will be determined likewise to what has been done in Section 3.1.2. Note that the choice $\Psi_j = \Psi_1 (= 0)$ is optimal and that, as in Eq. (61), there are no even superharmonics, so that the reduced problems have the only variables h_j, $j = 3, 5, 7, \ldots, N$. Furthermore, the solution is again unique.

The first case $N = 3$, which is that considered in Ref. [38], corresponds to a single superharmonic, and can be solved analytically. The optimal solution has $h_3 = -1/6$ and the optimal gain is $G = 2/\sqrt{3} \cong 1.1547$. Contrary to the one-side control, with just one superharmonic it is possible to obtain more than one-half of the maximum theoretical gain, even if the upper bound is yet far. The successive problems have been solved with the same numerical tool of Section 3.1.2; the constraint $-\min\{h(m)\} = \max\{h(m)\}$ is automatically satisfied by the combination of odd superharmonics, so that there is no need to further modify the algorithm. The results are reported in Table 2, which clearly shows that also in this case the reduced order solutions tend to the mathematical solution of Section 3.2.1 when $N \to \infty$.

3.2.3. On the constrained problem with infinite number of superharmonics

The guidelines and ideas of Section 3.1.3 are used in this section to obtain the solution of the problem with infinite superharmonics. The same constraint (49) is considered to assure convergence of the series representing the optimal excitation, and the main difference with the analysis of Section 3.1.3 is that only odd superharmonics are involved in the present case.

By using inequalities (49) one obtains

$$\begin{aligned} h(m) &= \cos(m + \psi_1) + \textstyle\sum_{j=2}^{\infty} h_{(2j-1)} \cos[(2j-1)m + \Psi_j] \\ &\leqslant \cos(m + \psi_1) + A \textstyle\sum_{j=2}^{\infty} a^{2j-1} = \cos(m + \psi_1) + A \dfrac{a^3}{1 - a^2}, \end{aligned} \tag{62}$$

so that

$$\min_{m \in [0, 2\pi]} \{h(m)\} \leqslant -1 + A \frac{a^3}{1 - a^2}, \tag{63}$$

Table 2
The numerical results of various optimization problems with increasing finite number of superharmonics in the case of global control of symmetric systems

N	G_N	h_3	h_5	h_7	h_9	h_{11}	h_{13}	h_{15}
3	1.1547	−0.166667						
5	1.2071	−0.232259	0.060987					
7	1.2310	−0.264943	0.100220	−0.028897				
9	1.2440	−0.284314	0.125257	−0.053460	0.016365			
11	1.2518	−0.296177	0.141769	−0.071125	0.031854	−0.009969		
13	1.2568	−0.304101	0.153247	−0.083936	0.044376	−0.020352	0.006420	
15	1.2597	−0.307322	0.156798	−0.087358	0.047836	−0.024047	0.010154	−0.002998
∞	1.2732	−0.333333	0.200000	−0.142857	0.111111	−0.090909	0.076923	−0.066667

or, remembering that $G = -1/\min\{h(m)\}$,

$$G \leqslant \frac{1}{1 - Aa^3/(1-a^3)}, \tag{64}$$

which shows that the right hand side is a (constrained) upper bound for the optimal gain G. Summing up Eq. (64) with the unconstrained upper bound $G \leqslant 4/\pi$, it is possible to obtain the following overall bound for the optimal gain:

$$G \leqslant \begin{cases} 4/\pi & \text{if } A > \dfrac{1-a^2}{a^3}\left(1 - \dfrac{\pi}{4}\right), \\ \dfrac{1}{1 - \dfrac{Aa^3}{1-a^2}} & \text{if } A < \dfrac{1-a^2}{a^3}\left(1 - \dfrac{\pi}{4}\right), \end{cases} \tag{65}$$

which is illustrated in Fig. 8 for various values of A. As in Eq. (53), the constrained upper bound reduces the unconstrained upper bound only for medium and low values of a, i.e., for medium and large values of ω, where the exact solution can be determined.

The test function

$$h(m) = \cos(m) - A\sum_{j=2}^{\infty} a^{2j-1}\cos[(2j-1)m] = \cos(m) - Aa^3\frac{\cos(3m) - a^2\cos(m)}{1 - 2a^2\cos(2m) + a^4} \tag{66}$$

satisfies constraints (49). For

$$A \leqslant \frac{(1-a^2)^3}{a^3(a^4 - 2a^2 + 9)}, \tag{67}$$

the minimum (attained for $m = \pi$) is $-1 + Aa^3/(1-a^2)$, and the associated gain is

$$G = \frac{1}{1 - Aa^3/(1-a^2)}. \tag{68}$$

Comparing Eq. (68) with Eq. (65) it is possible to see that the gain associated with the test function (66) coincides with the constrained upper bound, and this proves the following proposition:

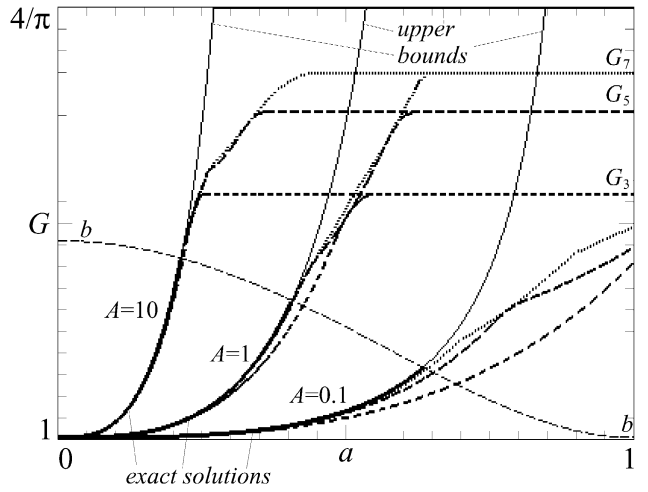

Fig. 8. The upper bound (65) of the optimal gain G for various values of A. The solid thick lines are the exact solutions of Proposition 2, while the line b–b delimits the range of validity of the exact solutions, and is given by Eq. (69). The other thick lines are the reduced (constrained and unconstrained) optimal gains G_3, G_5 and G_7, respectively.

Proposition 2. *In range* (67), *function* (66) *is a solution of problem* (59) *under constraint* (49).

The optimal gains (68) associated with the solution of Proposition 2 are depicted with solid lines in Fig. 8 for various values of A. The line b–b, on the other hand, delimitates the range of validity of the exact solutions, and is obtained by substituting the limit value of A, given by Eq. (67) with the equality sign, in Eq. (68), thus providing the limiting value of the exact G

$$\frac{a^4 - 2a^2 + 9}{8}. \tag{69}$$

3.2.4. On the constrained problems with finite but bounded number of superharmonics

This section is the companion, for global control, of Section 3.1.4, and has the same motivations.

The reduced optimal solution with N terms satisfies constraints (49) as long as

$$a \geqslant |h_{(2j-1)}/A|^{[1/(2j-1)]}, \quad j = 2, 3, \ldots, (N+1)/2, \tag{70}$$

where the $h_{(2j-1)}$ are reported in Table 2. The first case $N = 3$ can be solved analytically. One has $G_3 = 2/\sqrt{3}$ and $h_3 = -1/6$ for $(6A)^{(-1/3)} < a$, $G_3 = 3\sqrt{3Aa^3}/(1 + 3Aa^3)^{(3/2)}$ and $h_3 = -Aa^3$ for $(9A)^{(-1/3)} < a < (6A)^{(-1/3)}$, $G_3 = 1/(1 - Aa^3)$ and $h_3 = -Aa^2$ for $a < (9A)^{(-1/3)}$. The curve $G_3 = G_3(a)$ is reported in Fig. 8 for various values of A.

The other cases $N > 3$ have been solved numerically with the same method as in Section 3.1.2, by accounting for constraints (49) through a penalty term added to the functional, and the resulting functions $G_N = G_N(a)$ are also reported in Fig. 8. Note how for an increasing number of

superharmonics the curves accumulate quite fast on a corresponding curve which represents the optimal solution of the constrained optimal problem with infinite superharmonics.

4. Conclusions

An extensive theoretical analysis has been carried out to illustrate the *generic* features of a method for controlling non-linear dynamics and chaos previously developed by the authors for different mechanical systems, separately. Several softening and symmetric hardening 1-d.o.f. oscillators, characterized by the presence of a homo/heteroclinic bifurcation playing a central role in the dynamics organization and evolution, have been analyzed. Based on this common dynamic behaviour, a control method aimed at avoiding those bifurcations has been analyzed and discussed in-depth in a *unified* context.

The analysis has been developed in a theoretical framework by means of the Melnikov's method, which permits the analytical detection of homo/heteroclinic bifurcations in the case of small damping and excitation. While allowing for a proper frameworking of the control procedure within the overall scenario of system dynamics, the analytical approach is not actually a peculiarity of the method, which indeed can be applied to any kind of homo/heteroclinic bifurcation, possibly detected numerically [34].

The global bifurcations have been removed in an optimal way by selecting, for fixed frequency and amplitude, the best *shape* of the excitation permitting the maximum shift of the critical event in parameter space. In the case of more than one homo/heteroclinic bifurcation, one can choose to control either one single bifurcation (one-side controls) or all of the bifurcations simultaneously (global control). Each of these different approaches leads to a related mathematical problem of optimization. It has been shown that there is only *one* optimization problem, under a system-independent constraint in the case of global control. This constitutes an important *unifying* feature of the control method.

The obtained mathematical problem is just the same as found for the inverted pendulum [17]. This ensues from the common dynamical root shared by strongly non-linear (smooth) and piecewise linear (discontinuous) systems, which is reflected in the generic nature of the control method, irrespective of the system which it is applied to. This permits conjecture that applying the method to further systems would lead again to the same optimization problem, with possibly minor technical differences.

The mathematical problem has been discussed and solved in various forms. The exact solution in the case of infinite superharmonics has been found, and it has been shown that it is physically inadmissible, because it gives a divergent Fourier representation of the optimal excitation. Thus, other schemes have been developed to overcome this drawback. In particular, reduced (i.e., with finite number of superharmonics), constrained (with a further constraint introduced in the optimization problem to account for physical admissibility) and reduced/constrained solutions have been obtained numerically and analytically. It is worth remarking that, in any case, the physical admissibility is expressed by the same mathematical constraint, thus further confirming the generality of the method.

Of course, it is necessary to verify whether the control procedure actually works for the considered systems. This is shown by the satisfactory performances highlighted in the numerical

analysis of the impact inverted pendulum [18], of the Helmholtz oscillator [13] and of the hardening Duffing oscillator [19].

All of the obtained optimal solutions are system independent. However, a basic difference occurs between symmetric and asymmetric hardening systems: the latter are seen to exhibit a singular behaviour characterized by a more involved scenario of global control and by system-dependent optimal solutions [23].

References

[1] J.M.T. Thompson, H.B. Stewart, *Nonlinear Dynamics and Chaos*, Wiley, New York, 1986.

[2] H. Troger, W. Szemplinska-Stupnicka (Eds.), *Engineering Applications of Dynamics of Chaos*, Springer, New York, 1991.

[3] F.C. Moon, *Chaotic and Fractal Dynamics. An Introduction for Applied Scientists and Engineers*, Wiley, New York, 1992.

[4] A.H. Nayfeh, B. Balachandran, *Applied Nonlinear Dynamics: Analytical, Computational, and Experimental Methods*, Wiley-Interscience, New York, 1995.

[5] G. Kovacic, S. Wiggins, Orbits homoclinic to resonance, with an application to chaos in a model of the forced and damped sine-Gordon equation, *Physica D* 57 (1992) 185–225.

[6] F.C. Moon, J. Cusumano, P.J. Holmes, Evidence for homoclinic orbits as a precursor to chaos in a magnetic pendulum, *Physica D* 24 (1987) 383–390.

[7] A. Katz, E.H. Dowell, From single well chaos to cross well chaos: a detailed explanation in terms of manifold intersections, *International Journal of Bifurcation and Chaos* 4 (1994) 933–941.

[8] J. Guckenheimer, P. Holmes, *Nonlinear Oscillations, Dynamical Systems, and Bifurcations of Vector Fields*, Springer, New York, 1983.

[9] S. Wiggins, *Global Bifurcation and Chaos: Analytical Methods*, Springer, New York, Heidelberg, Berlin, 1988.

[10] S. Wiggins, *Introduction to Applied Nonlinear Dynamical Systems and Chaos*, Springer, New York, Heidelberg, Berlin, 1990.

[11] J.M.T. Thompson, F.A. McRobie, Indeterminate bifurcations and the global dynamics of driven oscillators, in: E. Kreuzer, G. Schmidt (Eds.), *Proceedings of the First European Nonlinear Oscillations Conference*, Akademie Verlag, Berlin, Hamburg, August 16–20, pp. 107–128, 1993.

[12] J.M.T. Thompson, Chaotic phenomena triggering the escape from a potential well, *Proceedings of the Royal Society of London A* 421 (1989) 195–225.

[13] S. Lenci, G. Rega, Optimal control of homoclinic bifurcation: theoretical treatment and practical reduction of safe basin erosion in the Helmholtz oscillator, *Journal of Vibration and Control* 9 (2003) 281–316.

[14] R. Lima, M. Pettini, Suppression of chaos by resonant parametric perturbations, *Physical Review A* 41 (1990) 726–733.

[15] T. Kapitaniak, *Controlling Chaos*, Academic Press, Lodz, 1996.

[16] G. Chen, X. Dong, *From Chaos to Order: Methodologies Perspectives and Applications*, World Scientific Publications, Singapore, 1998.

[17] S. Lenci, G. Rega, A procedure for reducing the chaotic response region in an impact mechanical system, *Nonlinear Dynamics* 15 (1998) 391–409.

[18] S. Lenci, G. Rega, Controlling nonlinear dynamics in a two-well impact system, Parts I and II, *International Journal of Bifurcation and Chaos* 8 (1998) 2387–2424.

[19] S. Lenci, G. Rega, Optimal control of nonregular dynamics in a Duffing oscillator, *Nonlinear Dynamics* 33 (2003) 71–86.

[20] S. Lenci, R. Lupini, Homoclinic and heteroclinic solutions for a class of two dimensional Hamiltonian systems, *Zeitschrift fuer Angewandte Mathmatik und Physik (ZAMP)* 47 (1996) 97–111.

[21] K. Ide, S. Wiggins, The bifurcation to homoclinic tori in the quasiperiodically forced Duffing oscillator, *Physica D* 34 (1989) 169–182.

[22] P. Holmes, J. Marsden, A partial differential equation with infinitely many periodic orbits: chaotic oscillations of a forced beam, *Archive for Rational Mechanics and Analysis* 76 (1981) 135–165.
[23] S. Lenci, G. Rega, Global optimal control and system-dependent solutions in the hardening Helmholtz–Duffing oscillator, *Chaos, Solitons and Fractals* (2004), in press.
[24] F.A. McRobie, Birkhoff signature change: a criterion for the instability of chaotic resonance, *Philosophical Transactions of the Royal Society of London A* 338 (1992) 557–568.
[25] W. Szemplinska-Stupnicka, The analytical predictive criteria for chaos and escape in nonlinear oscillators: a survey, *Nonlinear Dynamics* 7 (1995) 129–147.
[26] J.M.T. Thompson, R.C.T. Rainey, M.S. Soliman, Mechanics of ship capsize under direct and parametric wave excitation, *Philosophical Transactions of the Royal Society of London A* 338 (1992) 471–490.
[27] K. Yagasaki, Chaos in a weakly nonlinear oscillator with parametric and external resonances, *American Society of Mechanical Engineers Journal of Applied Mechanics* 58 (1991) 244–250.
[28] J.M. Falzarano, S.W. Shaw, A.W. Troesch, Application of global methods for analyzing dynamical systems to ship rolling motion and capsizing, *International Journal of Bifurcation and Chaos* 2 (1992) 101–115.
[29] R. van Dooren, On the transition from regular to chaotic behaviour in the Duffing oscillator, *Journal of Sound and Vibration* 123 (1988) 327–339.
[30] A.H. Nayfeh, N.E. Sanchez, Bifurcations in a forced softening Duffing oscillator, *International Journal on Non-linear Mechanics* 24 (1989) 483–497.
[31] P. Hagedorn, *Nonlinear Oscillations*, Oxford University Press, New York, 1988.
[32] W.-Y. Tseng, J. Dugundji, Nonlinear vibrations of a buckled beam under harmonic excitation, *American Society of Mechanical Engineers Journal of Applied Mechanics* 38 (1971) 467–476.
[33] W. Szemplinska-Stupnicka, J. Rudowski, Steady state in the twin-well potential oscillator: computer simulations and approximate analytical studies, *Chaos* 3 (1993) 375–385.
[34] S. Lenci, G. Rega, Optimal numerical control of single-well to cross-well chaos transition in mechanical systems, *Chaos, Solitons and Fractals* 15 (2003) 173–186.
[35] S. Lenci, G. Rega, Global chaos control in a periodically forced oscillator, in: A.K. Bajaj, N.S. Namachchivaya, M.A. Franchek (Eds.), *Nonlinear Dynamics and Control*, *Proceedings of the American Society of Mechanical Engineers, International Mechanical Engineering Congress*, DE-Vol. 91, November 17–22, 1996, Atlanta, GA, USA, pp. 111–116.
[36] E.R. Hansen, *A Table of Series and Products*, Prentice-Hall, Englewood Cliffs, NJ, USA, 1975.
[37] J.A. Nelder, R. Mead, A simplex method for function minimization, *Computer Journal* 7 (1964) 308–313.
[38] S.W. Shaw, The suppression of chaos in periodically forced oscillators, in: W. Schiehlen (Ed.), *Nonlinear Dynamics in Engineering Systems*, *Proceedings of IUTAM Symposium*, Stuttgart, Germany, Springer, Berlin, August 21–25, 1989, pp. 289–296.